THE EFFECT OF CONTACT CONDITIONS AND MATERIAL PROPERTIES ON ELASTIC-PLASTIC SPHERICAL CONTACT

Victor Brizmer, Yuval Zait, Yuri Kligerman and Izhak Etsion

THE EFFECT OF CONTACT CONDITIONS AND MATERIAL PROPERTIES ON ELASTIC-PLASTIC SPHERICAL CONTACT

VICTOR BRIZMER, YUVAL ZAIT, YURI KLIGERMAN AND IZHAK ETSION

The elastic-plastic contact between a sphere and rigid flat is analyzed under perfect slip and full stick conditions for a wide range of the sphere mechanical properties. The analysis provides comparison of the contact load, contact area and distribution of the contact pressure for these two contact conditions. It is found that the contact conditions and mechanical properties have little effect on the global contact parameters. However, the evolution of the plastic zone with increasing interference is substantially different for contacts under perfect slip or full stick conditions.

Nomenclature

a = contact area radius

a_c = critical contact area radius: $\sqrt{R\omega_c}$ in slip, $\sqrt{R\delta_c}$ in stick

A = contact area

A_c = critical contact area: $\pi R\omega_c$ in slip, $\pi R\delta_c$ in stick

A^* = $A/\pi R\omega_c$ in slip, $A/\pi R\delta_c$ in stick

C_v = $p_{mc}/Y_0 = 1.234 + 1.256\nu$

E = Young's modulus of the sphere

E_T = tangent modulus of the sphere

L_c = critical load in stick

p = contact pressure

p_{av} = average contact pressure, P/A

p_{avc} = critical average pressure in slip, $(2/3)p_{mc}$

p_{mc} = critical maximum pressure in slip

P = load

P_c = critical load in slip

P^* = P/P_c in slip, P/L_c in stick

R = radius of the sphere

Y_0 = virgin yield strength of the sphere

z_0 = location of yielding inception

Keywords: spherical contact, contact conditions, elastic-plastic contact.

δ_c = critical interference in stick

ν = Poisson's ratio of the sphere

ω = interference

ω_c = critical interference in slip

ω^* = ω/ω_c in slip, ω/δ_c in stick

ω_t = transition interference, at which the plastic region first reaches the sphere surface

ω_t^* = ω_t/ω_c in slip, ω_t/δ_c in stick

ζ_0 = dimensionless yielding inception depth, z_0/a

ζ_0^* = yielding inception depth ratio (stick over slip).

1. Introduction

The elastic-plastic contact of a deformable sphere and a rigid flat is a primary problem in contact mechanics with important scientific and technological aspects. The subject stems from the classical work of Hertz in 1881, who derived an analytical solution for the frictionless (that is, perfect slip) elastic contact of two spheres [Johnson 1985]. The stress field associated with elastic spherical contact was calculated in detail by Huber in 1904 [Fischer-Cripps 2000]. These pioneering works were extended in the following years to expand the frictionless contact into the elastic plastic regime, and to include frictional contact.

Chang et al. [1987] developed a model (CEB model) for the elastic-plastic contact between rough surfaces, which was based on analyzing the contact between a single sphere and a rigid flat under perfect slip condition. According to this model the sphere remains elastic, and hence the theory of Hertz holds until a certain critical interference at which yielding inception in the sphere is reached. Above the critical interference volume conservation of the sphere summit is imposed while the contact pressure distribution is assumed uniform and equal to the maximum pressure at the yielding inception. This simplified model resulted in a discontinuity in the contact load and in the derivative of the contact area with respect to the interference at the transition from elastic to elastic-plastic regime. Several modifications of the original CEB model were suggested [Evseev et al. 1991; Chang 1997; Zhao et al. 2000] in order to smooth the transition from the elastic to plastic regime, However, all these modifications are purely mathematical manipulations without any physical basis. Mesarovic and Fleck [2000] analyzed the problem of a normal frictionless contact between two dissimilar spheres. They studied the effect of material strain-hardening and the geometrical and mechanical dissimilarity of the spheres on the contact parameters and on the regime of deformation. Kogut and Etsion [2002] used a finite element method to study numerically the evolution of the plastic zone in elastic-plastic contact between a sphere and a rigid flat under perfect slip condition. They provided convenient dimensionless expressions for the contact load, contact area and mean contact pressure, covering a wide range of interferences for a single value of the Poisson's ratio ($\nu = 0.3$). Similar results were then obtained by Quicksall et al. [2004] and Jackson and Green [2005]. Etsion et al. [2005] studied the process of loading-unloading of an elastic-plastic loaded sphere in contact with a rigid flat under perfect slip condition. They calculated the contact load, stresses and deformations in the sphere during both loading and unloading, for a wide range of interferences and several combinations of material properties.

The first analytical solution of the elastic spherical contact problem under full stick condition is by Goodman [1962]. Goodman found a simplified solution for the tangential stress distribution over the contact area of two dissimilar elastic spheres. The effect of these tangential stresses on the normal displacements was neglected, so that the pressure distribution over the contact area was assumed to be Hertzian. A more exact analysis of the elastic spherical contact under full stick contact condition was performed by Spence [1968] who solved simultaneously the dual integral equations for shear stresses and pressure distribution over the contact area and calculated the total compressive load. It follows from Spence's results that for small values of Poisson's ratio, the influence of the shear stresses on the contact load is appreciable. Spence [1975] extended his previous analysis to the case of partial stick using a certain value of friction coefficient. Hills and Sackfield [1987] presented a complete picture of the stress distribution in the elastic spherical contact under full and partial stick contact conditions, using the assumptions of [Goodman 1962]. Kosior et al. [1999] analyzed an elastic spherical contact under partial slip condition (with a finite Coulomb friction) using a domain decomposition method coupled with a boundary element method. They calculated stress distribution, contact radius and displacement as functions of the sphere mechanical properties. Their results were in good agreement with the analytical solution of Spence [1975]. Mesarovic and Fleck [1999] studied numerically the problem of spherical indentation of a rigid sphere into an elastic-plastic half-space under perfect slip and full stick conditions. They investigated the effect of contact conditions and material strain-hardening on the contact parameters and on the regime of deformation. Brizmer et al. [2006] studied the influence of the two different contact conditions (full stick vs. perfect slip) and material properties on the elasticity terminus of a contact between a smooth elastic sphere and rigid flat. The plastic yield inception of ductile materials and the failure inception of brittle materials were studied separately.

From the above introduction it can be seen that most of the existing literature on elastic-plastic spherical contact concerns perfect slip condition while full stick condition is mostly limited to elastic contact. Moreover, an accurate study of the effect of the sphere mechanical properties on the contact parameters, such as contact load and contact area, and on the evolution of the plastic zone with increasing interference, is still missing. Since a realistic elastic-plastic contact of a sphere and flat may be far from the ideal assumption of perfect slip, it seems appropriate to analyze the problem of spherical contact under stick condition for different material properties, and to compare the results with the corresponding solutions of perfect slip.

2. Theoretical background

Figure 1 presents a deformable sphere in contact with a rigid flat. The solid and dashed lines show the contours of the contacting bodies after and before the loading. The inner solid contour of the deformed sphere shown in Figure 1 corresponds to relatively low values of Poisson's ratio (that is, a compressible material), when the volume of the sphere diminishes under compressive loading. For high values of Poisson's ratio (that is, a nearly incompressible material) the volume of the sphere remains almost constant during the deformation. For conservation of volume, the points of the sphere will tend to move outwards rather than inwards in the radial direction (the outer solid contour in Figure 1). Two different types of the contact conditions are analyzed in the present work: perfect slip and full stick. The former case assumes no tangential stresses in the contact area. The latter case implies that corresponding
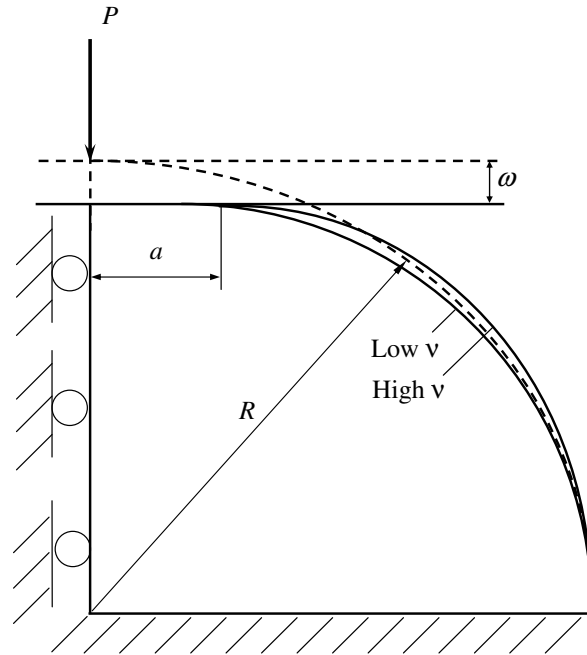
Figure 1. Model of a deformable sphere in contact with a rigid flat.

points of the sphere and the flat (which initially laid outside the contact area and were free to acquire a relative displacement) that are overtaken by the expanding contact zone, are prevented from further relative displacement [Johnson et al. 1973]. The perfect slip assumption, although not describing a general realistic contact condition, allows a relatively simple analytical solution in the elastic regime and can be considered as a limiting case. The full stick assumption, on the other hand, is more realistic when considering the junction formed in the interface of contacting bodies [Tabor 1959]. In this case the stress field and yielding criterion at the junction interface obey material constitutive laws. This approach is different from previous frictional contact solutions (for example, [Spence 1975]) where partial slip is obtained when a certain local Coulomb friction law is assumed.

The contact area, its radius a, and interference ω (see Equation (1)) correspond to a contact load P. The material of the sphere is assumed to be elastic-isotropic linear hardening [Etsion et al. 2005].

Since the problem is axisymmetric, it is sufficient to consider only half of the axisymmetric hemisphere section, as shown in Figure 1. The boundary conditions consist of constraints in the vertical and radial directions at the bottom of the hemisphere and in the radial direction at the axis of symmetry (see Equation (1)). The surface of the sphere is free elsewhere except for tractions imposed by the contacting rigid flat.

The critical interference ω_c or δ_c at yielding inception in perfect slip or in full stick, respectively, and their corresponding values of the critical loads, P_c and L_c, were given by Brizmer et al. [2006] in the

form:

$$\omega_c = \left(C_\nu \frac{\pi(1-\nu^2)}{2} \left(\frac{Y_0}{E} \right) \right)^2 R \tag{1}$$

$$\delta_c/\omega_c = 6.82\nu - 7.83(\nu^2 + 0.0586) \tag{2}$$

$$P_c = \frac{\pi^3 Y_0}{6} C_\nu^3 \left(R(1-\nu^2) \left(\frac{Y_0}{E} \right) \right)^2 \tag{3}$$

$$L_c/P_c = 8.88\nu - 10.13(\nu^2 + 0.089). \tag{4}$$

In Equations (1) and (3), $C_\nu = 1.234 + 1.256\,\nu$ is the maximum dimensionless contact pressure at yielding inception in slip, p_{mc}/Y_0. The parameters Y_0, E, and ν are the virgin yield stress, the Young modulus, and the Poisson's ratio of the sphere material, respectively. Equations (1) and (3) for the perfect slip were obtained analytically, using the Hertz solution [Johnson 1985] and applying the von Mises yield criterion. Equations (2) and (4), corresponding to the full stick condition, were derived numerically.

The critical value of the contact area, corresponding to yield inception for slip contact condition follows from Hertz solution [Johnson 1985]:

$$A_c = \pi \omega_c R \tag{5}$$

and for stick, as was found in [Brizmer et al. 2006]:

$$A_c = \pi \delta_c R. \tag{6}$$

The dimensionless yielding inception depth in perfect slip, ζ_0, and the ratio of yielding inception depth in stick over that in slip, ζ_0^*, are [Brizmer et al. 2006]:

$$\zeta_0 = z_0/a = 0.381 + \nu/3 \tag{7}$$

$$\begin{aligned} \zeta_0^* &= 0, \ \nu \le 0.26; \\ \zeta_0^* &= 1.54(\nu - 0.26)^{0.294}, \ 0.26 < \nu \le 0.5; \end{aligned} \tag{8}$$

where z_0 is the yielding inception depth in perfect slip.

3. Finite elements model

The loading of an elastic-plastic contact is a complicated problem. To avoid oversimplifications, this contact problem was solved numerically, by a finite element method using the commercial package AN-SYS 8.0. The mesh consisted of 8,800 six-node triangular axisymmetric elements (Plane2) comprising a total of 29,277 nodes. The sphere was divided into three different mesh density zones (see Figure 2), where zones I and II were within $0.015R$ and $0.1R$, respectively, from the sphere summit, and zone III outside the $0.1R$ distance. Zone I had the finest mesh and the other zones had a gradually coarser mesh at increasing distance from the sphere summit. The sphere surface consisted of contact elements (Conta172) that matched the size of the elements in each zone. The rigid flat was modeled by a single nonflexible element (Targe169). The material of the sphere was assumed elastic linear isotropic hardening with a tangent modulus, E_T, that was selected as 2% of the Young modulus E, which is an upper limit of many
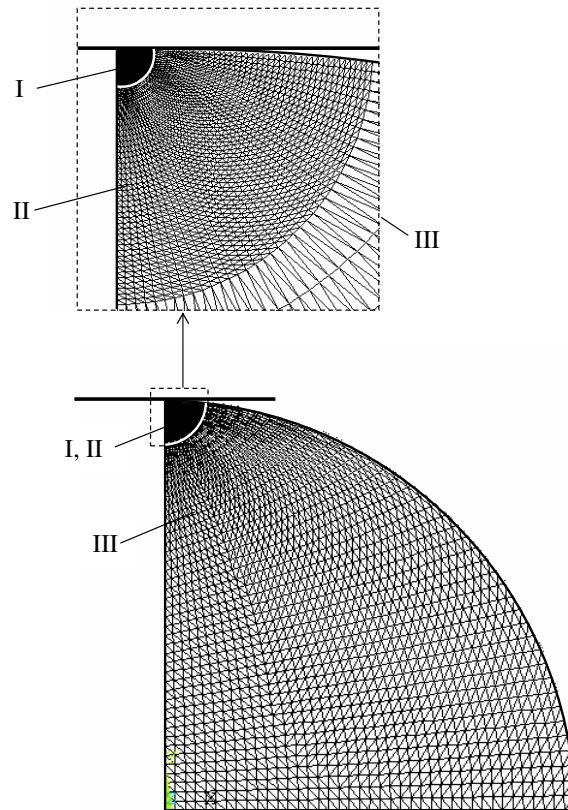
Figure 2. The finite elements model.

practical materials, see, for example, [Carmichael 1955]. This linear isotropic hardening significantly improves convergence compared to an elastic perfectly plastic material without causing much change (less than 2.5%) in the results. Hence, this hardening enables comparison with existing results for perfect slip condition, such as those in [Kogut and Etsion 2002], yet provides a better convergence of the numerical solution. The von Mises yielding criterion was used to detect local transition from elastic to plastic deformation, and Hooke's and the Prandtl–Reuss' constitutive laws governed the stress-strain relations in the elastic and plastic zones, respectively. A nonlinear finite deformation definition was used to allow large interferences (up to $\omega^* = 110$).

To verify the accuracy of the finite element model, results for purely elastic contact under perfect slip condition were tested against the Hertz solution. The correlations of the contact load and contact area were within 1% and 3%, respectively. Another check was done at high interferences in full stick and in perfect slip by increasing the mesh density and ensuring convergence of the results within a small pre-defined tolerance. Typical computation times on a 1.6 GHz PC were about 2–3 minutes for small, and 10–15 minutes for large interferences.

4. Results and discussion

The effects of the contact conditions (full stick vs. perfect slip), and of the material properties on the contact load and contact area were investigated in the present work over a wide range of dimensionless interferences from elastic to full plastic contact $0.25 \leq \omega^* \leq 110$ (here ω^* is ω/ω_c in slip and ω/δ_c in stick). Three different values of Poisson's ratio typical for ductile metals, 0.25, 0.35 and 0.45, were selected in the present analysis along with three values of the ratio E/Y_0: 500, 1000 and 2000. Each combination of the material properties was examined over the full range of interferences.

The results for the dimensionless contact load and contact area in slip as functions of ω^* in the elastic regime, $\omega^* < 1$, were found identical to the Hertz solution, as would be expected. The results of the contact area in stick were found to be identical to those in slip. From the Hertz solution $A = \pi R \omega$, hence, from the definition of the critical areas in slip and stick in Equations (5) and (6), respectively, it is clear that $A^* = A/A_c = \omega^*$ in both stick and slip regardless of the Poisson's ratio. The results of the contact load, P^*, in stick (P/L_c) were found very similar to these in slip (P/P_c) particularly at an increasing Poisson's ratio. The diminishing difference between the contact load P^* in stick and slip with an increasing Poisson's ratio is attributed to the increasing material incompressibility. This can be seen, at least for the elastic regime, from the Hertz solution for the radial displacement, u_r, of the sphere points at the contact area:

$$u_r(r, v) = f(r) \cdot (1 - 2v)(1 + v), \tag{9}$$

where $f(r)$ is a certain function of the radial coordinate, the radius of the contact area and the Young's modulus of the sphere. From Equation (9) it is clear that a higher Poisson's ratio results in lower relative displacements between the sphere and the flat in slip, making the slip condition closer to the zero relative displacements in stick condition.

In the elastic-plastic regime, $\omega^* > 1$, the numerical results for the dimensionless contact area A^* and contact load P^* as functions of ω^* were again very similar in stick and in slip. These results were best fitted and have the following forms:

$$A^* = \omega^* \left(1 + \exp \left(\frac{1}{1 - (\omega^*)^\alpha} \right) \right), \tag{10}$$

$$P^* = (\omega^*)^{3/2} \left(1 - \exp \left(\frac{1}{1 - (\omega^*)^\beta} \right) \right), \tag{11}$$

where α and β are linear functions of the Poisson's ratio:

$$\alpha = 0.25 + 0.125v; \qquad \beta = 0.174 + 0.08v.$$

The approximate expressions in Equations (10) and (11) for A^* and P^* describe the numerical FEM results with an average difference of 4% in A^* and 2% in P^*.

From Equation (10) it can be seen that for ω^* slightly larger than one (that is, just after the yielding inception), A^* approaches ω^*, in agreement with the elastic solution of Hertz. On the other hand, for large values of ω^*, A^* approaches $2\omega^*$, i.e. the approximate fully plastic solution of [Abbott and Firestone 1933]. Equation (11) gives $P^* \approx (\omega^*)^{3/2}$ for ω^* slightly larger than 1, which is in agreement with Hertz solution. These results compare favorably with the relevant dimensionless expressions presented
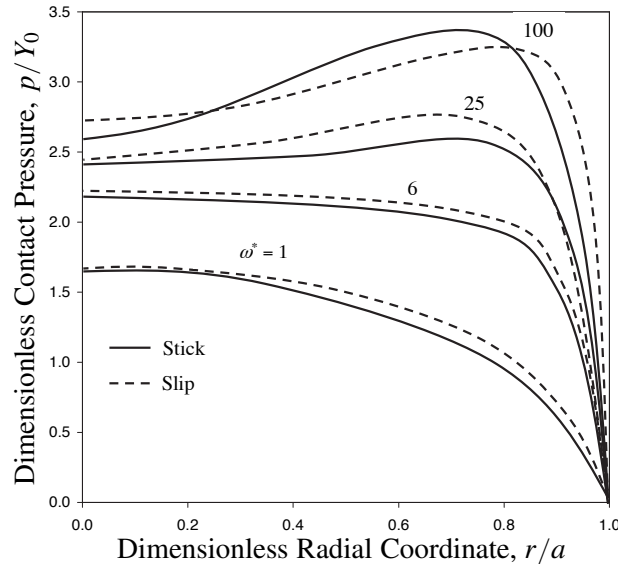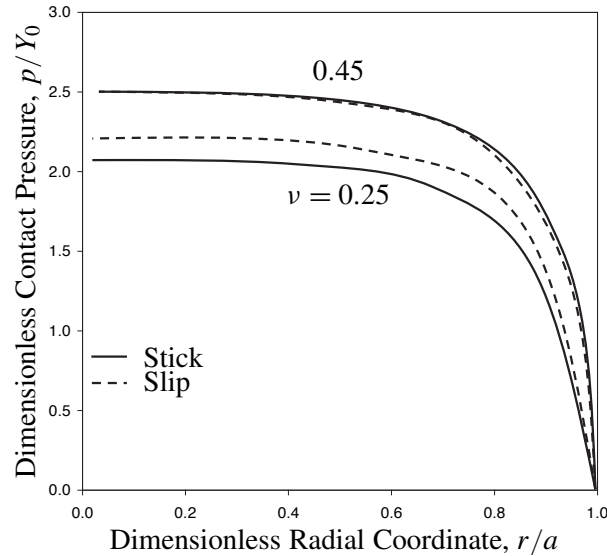
Figure 3. The effect of dimensionless interference on the dimensionless contact pressure distribution, p/Y_0, in slip and in stick, for a typical case of $\nu = 0.3$.

in [Kogut and Etsion 2002] (the KE model) and in [Etsion et al. 2005] for $\nu = 0.3$, and slip condition for elastic perfectly plastic and for elastic linear hardening materials, respectively.

Equations (10) and (11) suggest that normalizing the results for the contact area and contact load by their appropriate critical values at yielding inception for either slip or stick (see Equations (1) to (6)) as given by [Brizmer et al. 2006], provides, for ductile materials, a powerful universal solution for the elastic-plastic contact problem in both stick and slip where an analytical solution is impossible. It extends the classical Hertz solution into the elastic-plastic regime while providing a physical insight of the main dimensionless parameters affecting this contact problem in both slip and stick.

It can be seen from Equations (10) and (11) that the ratio E/Y_0 has no effect on the results for a given dimensionless interference ω^* in both stick and slip, while the Poisson's ratio has little effect on the dimensionless contact area and contact load. It is also evident that isotropic linear hardening has negligible effect on the results compared to elastic perfectly plastic behavior.

The effect of the contact conditions on the contact pressure distribution, p/Y_0, at the contact area for a typical case $\nu = 0.3$ is shown in Figure 3. The solid and dashed lines correspond to full stick and perfect slip, respectively. It can be seen that the two contact conditions yield very similar results for the full range of interferences with pressures in slip slightly higher than in stick, at least for $\omega^* \leq 25$. This seemingly counterintuitive result is due to the fact that the critical interference in stick δ_c is significantly less than ω_c in slip (e.g. $\delta_c/\omega_c \approx 0.88$ for $\nu = 0.3$, see Equation (2)). Hence, the pressure distributions in slip correspond to dimensional interference, ω, that is 12% higher than the dimensional interference in stick for a given value of ω^*. In other words, the pressure in slip would be somewhat lower than that in stick for the same dimensional interference. Recalling that the contact area depends on the interference (same contact area for same ω in both slip and stick), the results in Figure 3 are in agreement with the

Figure 4. The effect of the Poisson's ratio on the dimensionless contact pressure distribution in slip and in stick for the case of $\omega^* = 6$.

observation (see, for example, [Johnson 1985, p. 123]) that "friction can increase the total load required to produce a contact of given size by at most 5% compared with Hertz".

The effect of the Poisson's ratio on contact pressure distribution in slip and in stick is shown in Figure 4 for the case of $\omega^* = 6$. It can be seen that a higher Poisson's ratio results in higher contact pressure for this dimensionless interference in both slip and stick. This is attributed to the fact that at a higher Poisson's ratio, the material is less compressible and so higher pressure is required to deform it. For the case of $\nu = 0.45$ where the critical interferences in stick and slip are almost identical, as in Equation (2) (ω values in stick and in slip are equal), the solid and dashed lines coincide, that is, the pressure distributions in slip and in stick are almost identical. On the other hand, for $\nu = 0.25$ where $\delta_c/\omega_c \approx 0.76$ (see Equation (2)) the dimensional interference, ω, in slip for a given value of ω^* is larger than that in stick causing the pressure distribution in slip to be slightly higher than that in stick.

The dimensionless average contact pressure, p_{av}/Y_0, vs. the dimensionless interference, ω^*, in slip has the form (see Equations (1), (3), and (5) and the definition of C_ν):

$$\left(\frac{p_{av}}{Y_0}\right)_{\text{slip}} = \frac{P}{AY_0} = \frac{P^*}{A^*} \cdot \frac{P_c}{\pi \omega_c R Y_0} = \frac{P^*}{A^*} \cdot \frac{p_{avc}}{Y_0}, \tag{12}$$

while in stick:

$$\left(\frac{p_{av}}{Y_0}\right)_{\text{stick}} = \frac{P^*}{A^*} \cdot \frac{L_c}{\pi \delta_c R Y_0} = \frac{P^*}{A^*} \cdot \frac{p_{avc}}{Y_0} \cdot \frac{(L_c/P_c)}{(\delta_c/\omega_c)}, \tag{12a}$$
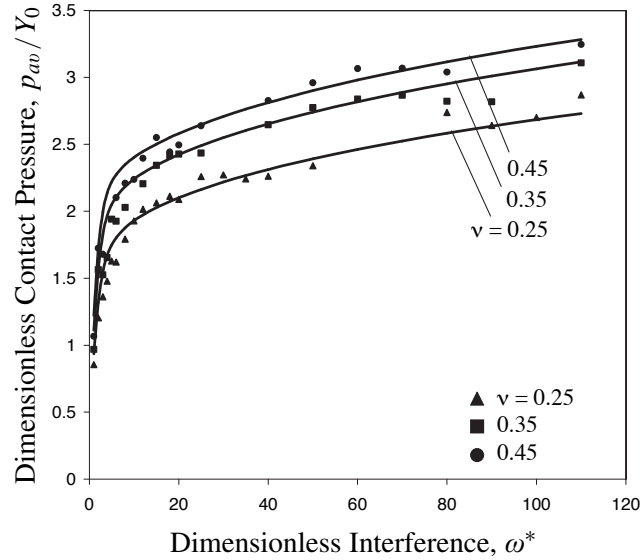
Figure 5. The dimensionless average contact pressure p_{av}/Y_0 vs. the dimensionless interference.

where the dimensionless parameters: p_{avc}/Y_0, L_c/P_c and δ_c/ω_c are known functions of ν (see Nomenclature and Equations (2) and (4)). From Equations (12) and (12a) we have:

$$\frac{(p_{av})_{\text{slip}}}{(p_{av})_{\text{stick}}} = \frac{\delta_c/\omega_c}{L_c/P_c}. \tag{13}$$

By using Equations (2) and (4) it can easily be shown that for $\nu = 0.25$, the ratio of the average contact pressures, slip over stick, in Equation (13) is 1.1, while for $\nu \geq 0.3$ it is very close to a unity. Hence, like the dimensionless contact area and contact load (Equations (10) and (11)), the average contact pressures in stick and in slip are very similar and can also be properly normalized by their critical values.

Substituting A^* and P^* from Equations (10) and (11), respectively, into Equation (12) or (12a) yields the dimensionless average pressure in stick or in slip as a function of ω^* and ν. The results are presented in Figure 5 along with the numerical FEM results showing a very good agreement with an average difference of 4%. It was found that Equations (12) or (12a) can also be well approximated by the simpler form:

$$\frac{p_{av}}{Y_0} = (\omega^*)^{1/2} \cdot \tanh\left(\frac{1}{2\big((\omega^*)^\gamma - 1\big)}\right) \cdot \frac{p_{avc}}{Y_0}, \tag{14}$$

where

$$\gamma = 0.2 + 0.06\nu,$$

without any loss of accuracy. It can be easily seen that for ω^* slightly larger than 1, $p_{av}/p_{avc} = (\omega^*)^{1/2}$, which is in agreement with the Hertz solution.

From Figure 5 it can be seen that the average contact pressure increases sharply up to an interference that is about $10\omega^*$. From there on the rate of increase of the average pressure diminishes, and at about $110\omega^*$ the average pressure reaches a value that varies from $2.73Y_0$ for $\nu = 0.25$ to $3.28Y_0$ for $\nu = 0.45$.

Dimensionless Radial Coordinate, r/a_c
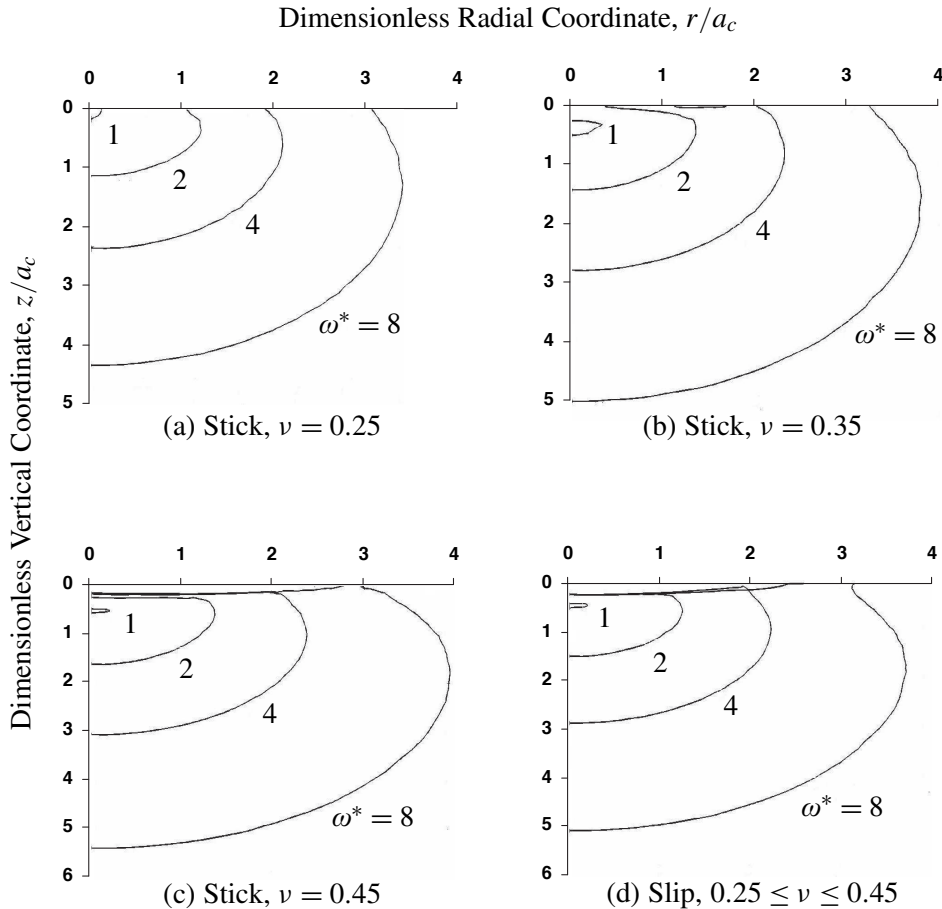
Figure 6. The early evolution of the plastic region for small values of the dimensionless interference in stick at different values of the Poisson's ratio (a)–(c) in comparison with that in slip for $0.25 \le \nu \le 0.45$ (d).

The higher average contact pressure at larger Poisson's ratios is due to the reduced compressibility as shown in Figure 4. The results in Figure 5 are in good agreement (within 5%) with [Kogut and Etsion 2002] where a value of $2.8Y_0$ was found for $\nu = 0.3$. A similar effect of the Poisson's ratio on the hardness was found by Kogut and Komvopoulos [2004] for indentation and Jackson and Green [2005]. In these two references a reduction in p_{av}/Y_0 was observed for very large interferences corresponding to a/R values in access of 0.1. Our analysis is limited to $a/R < 0.05$.

The early evolution of the plastic region for small dimensionless interferences ($\omega^* \le 8$) within the sphere tip is presented in Figure 6. As we see, the Poisson's ratio has a large effect on the early evolution of the plastic region under full stick condition (see Figure 6a–c). On the other hand it was found that under slip condition the Poisson's ratio effect is negligible. Hence, for slip condition just one typical case for the range $0.25 \le \nu \le 0.45$ is presented in Figure 6d. The differences in the early evolution of the
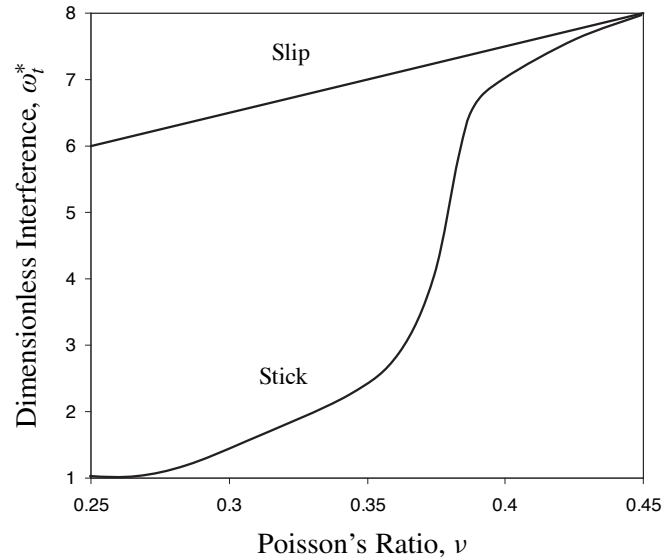
Figure 7. The dimensionless transition interference ω_t^*, for stick and for slip as a function of the Poisson's ratio.

plastic region between stick and slip are in good agreement with the results of [Brizmer et al. 2006] for the yielding inception depth that was found highly dependent on the Poisson's ratio in stick, but almost unaffected by it in slip (see Equations (7) and (8)). Another interesting difference between stick and slip concerns the existence of an elastic core close to the contact interface. This core is completely missing in Figure 6a, it has an annular shape in Figure 6b, and is continuous over a central portion of the contact area in Figures 6c and 6d. Further numerical simulations in the range $0.3 \leq \nu \leq 0.4$ revealed that this elastic core (that is, the elastic zone at the very top of the sphere surrounded by the expending plastic region), which persists up to relatively high values of ω^* in slip [Kogut and Etsion 2002], is completely missing in stick when $\nu < 0.35$. As can further be seen from Figure 6c, d the early evolution of the plastic region in stick for a Poisson's ratio of 0.45 is similar to that in slip.

The transition interference, ω_t^*, at which the evolving plastic zone first reaches the surface of the sphere is also very different in stick and in slip. This can be seen from Figures 6a–d, and more clearly from Figure 7. From this figure we see that in slip, ω_t^* varies linearly from 6 to 8 over the entire range of the Poisson's ratio. In stick, on the other hand, when $\nu \leq 0.26$ the plastic zone starts at the contact interface (see Equation (8) hence, $\omega_t^* = 1$. As the Poisson's ratio increases the transition interference, ω_t^*, in stick increases too, first moderately until $\nu = 0.35$, then very rapidly until $\nu = 0.39$, and finally as ν approaches 0.45 the transition interference in stick approaches that in slip. The higher values of ω_t^* in slip compared to stick, as shown in Figure 7, are due to the deeper location of yielding inception under the former contact condition (see Equations (7) and (8)), which requires more deformation for the plastic zone to reach the sphere surface. Also, at Poisson's ratios below 0.35 in stick, the plastic region first reaches the sphere surface at the center of the contact area even when incepting slightly below it (see Figures 6a and b). In slip this event starts close to the circumference of the contact area (see also [Kogut and Etsion 2002]) at a much longer distance from the point of yield inception and thus requires
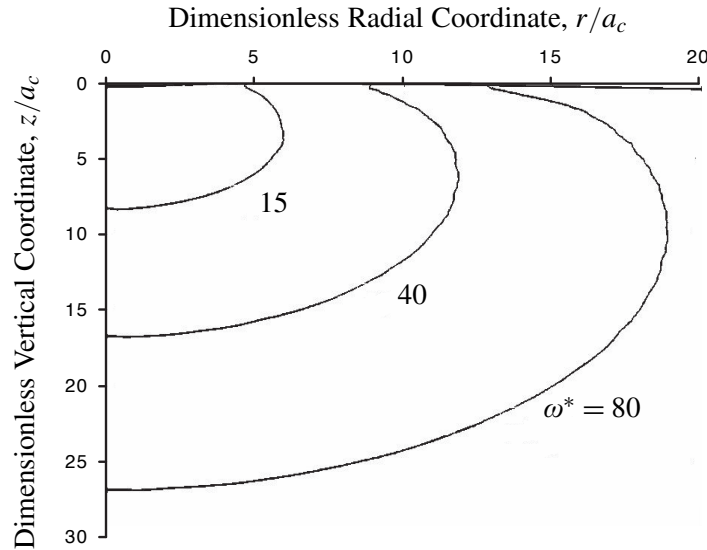
Figure 8. Typical evolution of the plastic zone for high values of the dimensionless interference for $0.25 \leq \nu \leq 0.45$, showing identical behavior in stick and slip.

larger interferences. The sharp increase of ω_t^* in stick observed above $\nu = 0.35$ can be explained by the appearance of the annular elastic core (see Figure 6b) that extends towards the center of the contact area with further increases of the Poisson's ratio (Figure 6c), blocking the upward advancement of the plastic zone front and forcing it radially out, similarly to the behavior in slip.

The evolution of the plastic zone for dimensionless interferences higher than 15 is shown in Figure 8. As can be seen the differences between stick and slip conditions disappear and the plastic zone becomes identical regardless of the Poisson's ratio. The reason for this identical behavior is that at higher interferences with increasing size of the plastic zone, the different historical location of the yielding inception and the development of the elastic core in stick and slip become insignificant.

5. Conclusion

The effects of contact condition (perfect slip or full stick) and material properties on elastic-plastic normally loaded spherical contact were investigated for a large range of interferences. The results for the dimensionless contact area, contact load and average contact pressure were found to be almost insensitive to the contact condition, independent of the ratios E/Y_0 and E_T/E and of the sphere radius, and slightly affected by the Poisson's ratio. The numerical results were approximated by simple empirical expressions based on realistic physical behavior. It was shown that normalizing the various parameters by their corresponding critical values at yielding inception provides a powerful general solution for the contact problem that is valid under both perfect slip and full stick conditions. Unlike the global contact parameters, the early evolution of the plastic zone in the contact region is very much affected by Poisson's ratio mainly under stick contact condition. Up to about $\nu = 0.4$ this evolution in stick is also very different

from the evolution in slip. At higher values of the Poisson's ratio the behavior in stick becomes very similar to that in slip. As the dimensionless interference increases and the plastic zone continues to expand, the differences between stick and slip diminish for the full range of Poisson's ratio.

References

[Abbott and Firestone 1933] E. J. Abbott and F. A. Firestone, "Specifying surface quantity – a method based on accurate measurement and comparison", *Mech. Eng.* **55** (1933), 569–572.

[Brizmer et al. 2006] V. Brizmer, Y. Kligerman, and I. Etsion, "The effect of contact conditions and material properties on the elasticity terminus of a spherical contact", *Int. J. Solids Struct.* **43**:18-19 (2006), 5736–5749.

[Carmichael 1955] C. Carmichael, *Kent's mechanical engineers' handbook: Design and production volume*, 12th ed., edited by C. Carmichael, Wiley, New York, 1955.

[Chang 1997] W. R. Chang, "An elastic-plastic contact model for a rough surface with an ion-plated soft metallic coating", *Wear* **212**:2 (1997), 229–237.

[Chang et al. 1987] W. R. Chang, I. Etsion, and D. B. Bogy, "An elastic-plastic model for the contact of rough surfaces", *J. Tribology* (*Trans. ASME*) **109** (1987), 257–263.

[Etsion et al. 2005] I. Etsion, Y. Kligerman, and Y. Kadin, "Unloading of an elastic-plastic loaded spherical contact", *Int. J. Solids Struct.* **42**:13 (2005), 3716–3729.

[Evseev et al. 1991] D. G. Evseev, B. M. Medvedev, and G. G. Grigoriyan, "Modification of the elastic-plastic model for the contact of rough surfaces", *Wear* **150**:1-2 (1991), 79–88.

[Fischer-Cripps 2000] A. C. Fischer-Cripps, *Introduction to contact mechanics*, Springer, New York, 2000.

[Goodman 1962] L. E. Goodman, "Contact stress analysis of normally loaded rough spheres", *J. Appl. Mech.* (*Trans. ASME*) **29** (1962), 515–522.

[Hills and Sackfield 1987] D. A. Hills and A. Sackfield, "The stress field induced by normal contact between dissimilar spheres", *J. Appl. Mech.* (*Trans. ASME*) **54** (1987), 8–14.

[Jackson and Green 2005] R. L. Jackson and I. Green, "A finite element study of elasto-plastic hemispherical contact against a rigid flat", *J. Tribology* (*Trans. ASME*) **127**:2 (2005), 343–354.

[Johnson 1985] K. L. Johnson, *Contact mechanics*, Cambridge University Press, Cambridge, MA, 1985.

[Johnson et al. 1973] K. L. Johnson, J. J. O'Connor, and A. C. Woodward, "The effect of the indenter elasticity on the hertzian fracture of brittle materials", *P. Roy. Soc. Lond. A Mat.* **A334** (1973), 95–117.

[Kogut and Etsion 2002] L. Kogut and I. Etsion, "Elastic-plastic contact analysis of a sphere and a rigid flat", *J. Appl. Mech.* (*Trans. ASME*) **69**:5 (2002), 657–662.

[Kogut and Komvopoulos 2004] L. Kogut and K. Komvopoulos, "Analysis of the spherical indentation cycle for elastic-perfectly plastic solids", *J. Mater. Res.* **19**:12 (2004), 3641–3653.

[Kosior et al. 1999] F. Kosior, N. Guyot, and G. Maurice, "Analysis of frictional contact problem using boundary element method and domain decomposition method", *Int. J. Numer. Methods. Eng.* **46**:1 (1999), 65–82.

[Mesarovic and Fleck 1999] S. D. Mesarovic and N. A. Fleck, "Spherical indentation of elastic-plastic solids", *P. Roy. Soc. Lond. A Mat.* **A455**:1987 (1999), 2707–2728.

[Mesarovic and Fleck 2000] S. D. Mesarovic and N. A. Fleck, "Frictionless indentation of dissimilar elastic-plastic spheres", *Int. J. Solids Struct.* **37**:46-47 (2000), 7071–7091.

[Quicksall et al. 2004] J. J. Quicksall, R. L. Jackson, and I. Green, "Elasto-plastic hemispherical contact models for various mechanical properties", *Proc. Inst. Mech. Eng.* **218**:4 (2004), 313–322. Part J: J. Eng. Tribol.

[Spence 1968] D. A. Spence, "Self-similar solutions to adhesive contact problems with incremental loading", *P. Roy. Soc. Lond. A Mat.* **A305**:1480 (1968), 55–80.

[Spence 1975] D. A. Spence, "The Hertz contact problem with finite friction", *J. Elasticity* **5**:3-4 (1975), 297–319.

[Tabor 1959] D. Tabor, "Junction growth in metallic friction: the role of combined stresses and surface contamination", *P. Roy. Soc. Lond. A Mat.* **A251**:1266 (1959), 378–393.

[Zhao et al. 2000] Y. Zhao, D. M. Maietta, and L. Chang, "An asperity microcontact model incorporating the transition from elastic deformation to fully plastic flow", *J. Tribology* (*Trans. ASME*) **122**:1 (2000), 86–93.

VICTOR BRIZMER: brizmer@technion.ac.il
Dept. of Mechanical Engineering, Technion, Haifa 32000, Israel

YUVAL ZAIT: syuvalza@t2.technion.ac.il
Dept. of Mechanical Engineering, Technion, Haifa 32000, Israel

YURI KLIGERMAN: mermdyk@technion.ac.il
Dept. of Mechanical Engineering, Technion, Haifa 32000, Israel

IZHAK ETSION: etsion@technion.ac.il
Dept. of Mechanical Engineering, Technion, Haifa 32000, Israel

JOURNAL OF MECHANICS OF MATERIALS AND STRUCTURES

http://www.jomms.org

See inside back cover or http://www.jomms.org for submission guidelines.

Journal of Mechanics of Materials and Structures